Ocean Dynamics (2018) 68:801–815
https://doi.org/10.1007/s10236-018-1160-x

Upper layer circulation, hydrography, and biological response of the Andaman waters during winter monsoon based on in situ and satellite observations

Salini Thaliyakkattil Chandran[1] · Smitha Bal Raj[2] · Sajeev Ravindran[1] · Sanjeevan Vellorkirakathil Narayana[2]

Received: 7 June 2017 / Accepted: 1 May 2018 / Published online: 25 May 2018

Abstract
Upper layer circulation, hydrography, and biological response of Andaman waters during winter monsoon are assessed based on the observations carried out onboard *FORV Sagar Sampada* during January 2009 and November–December 2011. Cool and dry air carried by the moderate winds (6 m/s) from north and northeast indicates the influence of northeast monsoon (NEM) in the area during the observation time. The characteristics of physical parameters and the water mass indicate that the southeastern side is dominated by the less saline water from South China Sea intruded through the Malacca Strait, whereas the northeast is influenced by the freshwater from Ayeyarwady-Salween river system. The western side of the Andaman and Nicobar Islands exhibits similar properties of Bay of Bengal (BoB) water as evidenced in the T-S relation. Circulation pattern is uniform for the upper 88 m and is found to be more geostrophic rather than wind driven. Magnitude of the current velocity varies between 100 and 900 mm/s in November–December 2011 with strong current (900 mm/s) near Katchal and Nancowry islands and 100 and 1000 mm/s in January 2009 recording strong current (1000 mm/s) near the Little Nicobar Island. The Andaman waters are observed as less productive during the season based on the satellite-derived surface chl-a (0.1–0.4 mg/m^3) and column-integrated primary productivity (PP) (100–275 mgC/m^2/d).

Keywords Hydrography · Upper layer circulation · VGPM · Geostrophy and Ekman

1 Introduction

The Andaman waters (surrounding the Andaman and Nicobar Islands) occupy the area between 6°–14°N and 91°–95°E in the eastern part of the North Indian Ocean. The northern part of the islands has got the wide continental shelf (170–200 km) and the continental slope along the eastern part of the islands is steeper than the western part (Murthy et al. 1981) and has erratic bottom topography. Sills are observed in the eastern side due to the sediment accumulation of Ayeyarwady River system (Ramaswamy et al. 2004). The abyssal plain (3000–4180 m) with an even floor is situated along the west coast of Andaman and Nicobar Islands. Preparis Channel (between Cape Negrais and North Andaman) in the north (200 m, 285 km wide), Ten Degree Channel (150 km wide) between Andaman and Nicobar Islands (1800 m), and Great Channel between Great Nicobar Island and Sumatra (> 1800 m and 189 km wide) connect the sea with Bay of Bengal (Sengupta et al. 1981; Kamesh Raju et al. 2004). The sea is also linked with South China Sea and Pacific Ocean through Malacca Strait at southeast. The main sources of freshwater to the northeast of Andaman and Nicobar Islands are Ayeyarwady (13.6 × 10^3 m^3/s), Salween rivers (6.69 × 10^3 m^3/s), and minor contributions from Sittang (1.59 × 10^3 m^3/s) and Tavoy rivers (Robinson et al. 2007). The other minor rivers in the Islands are Kalpong in North Andaman and Alexendra, Dagmar and Galathea river in Great Nicobar.

The Andaman waters experience the seasonally reversing Asian monsoons (Wyrtki 1973), summer monsoon during May–September, and winter monsoon during November–February. During northeast monsoon, the low saline water spread over the eastern side of the islands originates from the river discharge at north and the intrusion of low saline water from the South China Sea through the Malacca Strait at south (Ibrahim and Yanagi 2006). In addition, during the

Responsible Editor: Anthony C Hirst

✉ Salini Thaliyakkattil Chandran
salinitc@gmail.com

[1] Cochin University of Science and Technology, Kochi 682016, India

[2] Centre for Marine Living Resources & Ecology, Ministry of Earth Science, Kochi 682037, India

season, the region experiences strong evaporation of surface water due to cold dry continental air from the north. Thus, the area is a spot of deep air-sea interaction and associated convective activities and is marked as cyclone-prone area (Varkey et al. 1996). The presence of rivers and monsoonal winds influence the regional hydrography and circulation.

In addition to this, internal wave and tidal induced elevated vertical mixing is likely to influence the regional stratification and circulation pattern. The region is one of the sites where extraordinary large solitons have been observed (Osborne 1990; Hyder et al. 2005). Internal waves of extraordinary amplitude of 60 m, wavelength of 6–15 km, and speed > 2 m/s were noticed in this region (Alpers et al. 1997). This, together with longer period internal oscillation in the Northern Andaman Sea, produced the downward perturbation of the pycnocline. This also endorsed eastward-propagating Kelvin wave parallel to the continental slope. Such wave helped the mixing processes in the Andaman Sea (Hyder et al. 2005).

However, this region is least explored with regard to the oceanographic processes and the related biological impacts. Ramesh Babu and Sastry (1976) studied the hydrography of the sea during late winter. Small anticyclonic eddy around the Andaman Sea during premonsoon season (March) is reported by Unnikrishnan and Bahulayan (1991) using a two-dimensional vertically integrated model. Potemra et al. (1991) analyzed the seasonal circulation of the Andaman Sea using multilayer, adiabatic, numerical model and pointed out the propagation of Kelvin waves in Andaman Sea. Kelvin waves originating in the equatorial Indian Ocean follow the coastal waveguide counter clockwise around the perimeter of the Bay of Bengal (BoB) after reaching the Sumatra coast (Nienhaus et al. 2012)

Regarding biological production, the primary production of the area has been studied from the time of IIOE (International Indian Ocean Expedition). The region is characterized as oligotrophic when comparing the other areas of Indian Ocean (Bhattathiri and Devassy 1981), and maximum average column production is noticed during the southwest monsoon (586.73 mgC/m^2d) followed by northeast monsoon (440.68 mgC/m^2d) and inter-monsoon spring (319.19 mgC/m^2d) (Sarupriya and Bhargava 1993). The waters around the Andaman Islands are considered to be one of the major biodiversity hotspots in the Indian Ocean (Nair and Gireesh 2010). While studies from Geetha et al. (1997), analyzing the zooplankton of the upper column, explain that the seasonal biological production is high during winter monsoon, distribution and abundance of major mesozooplankton groups like amphipods, ostracods, copepods, and fish eggs and larvae are explained in many earlier studies (Manickasundaram and Ramaiyan 1990; Lalithambika Devi et al. 1996; Rosamma and Meenakshikunjamma 1996; Biju et al. 2010; Pillai et al. 2011).

The present study explains the seasonal response of the region to the prevailing physical mechanism, specifically the circulation pattern, hydrography, and the associated biology based on in situ and satellite observation during the winter monsoon January 2009 and November–December 2011. The study is formulated in the following aspects: (1) the hydrography and oceanography of the region, (2) the upper layer circulation pattern using ADCP, and (3) the physico-biological interactions in the primary level during winter monsoon.

2 Data and methodology

2.1 In situ data

In situ data were collected onboard *FORV Sagar Sampada* during 8–26 January 2009 and 21 November–14 December 2011 (Fig. 1).The transects are on the depths of 50, 100, 200, and 1000 m and the offshore station for which depth is greater than 1000 m. These datasets are used to understand the hydrography, circulation, and the associated biological responses in the Andaman waters. The meteorological parameters like air temperature, air pressure, and humidity are collected through the instruments/sensors attached to the Automated Weather Station (AWS) onboard in 1-min interval. Profiles of temperature, salinity, dissolved oxygen, and Sigma-t are obtained using SeaBird 911 plus CTD with Niskin water samplers and deck unit for data acquisition. It has four main sensors used to measure temperature, pressure, conductivity, and dissolved oxygen. The datasets are processed for 1 m bins. Salinity is also derived from water samples collected through Niskin samplers and using Guildline 8400A Autosal Salinometer to validate the CTD-derived data. Mixed layer depth (MLD) is derived from CTD profiles as the depth at which the seawater density (Sigma-t) exceeds the surface density by 0.2 kg/m^3 (Sprintall and Tomczak 1993). The isothermal layer depth (ILD), the depth of the top of the thermocline, is defined as the depth at which surface temperature decreases by 1 °C from sea surface temperature (Kara et al. 2000; Rao and Sivakumar 2003). The thickness of the barrier layer is computed as the difference between ILD and MLD (Lukas and Lindstrom 1991).

Vertical sections of currents are derived using hull mounted OS II BB ADCP of 76.8 kHz frequency operated along the ship's track with vertical range of operation between 30 and 400 m. Georeferencing is done in bottom track option along the coastal area (depth < 200 m), whereas navigation mode is opted for deeper areas. Current datasets are acquired using VmDas in 8 m bins and ensemble time of 2 s. The ship heading and navigational information are also recorded while acquiring the raw data. The first bin record of current started at 16 m depth. The data in earth coordinates were postprocessed

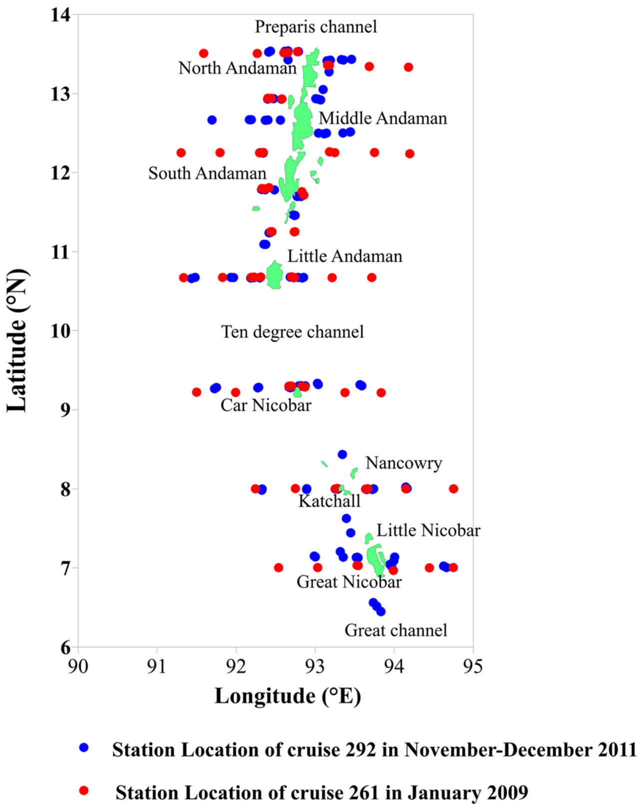

Fig. 1 Station location

using WinADCP, for an ensemble period of 1 min. Spurious values including the data at 16 m of currents were discarded from the data. Processed data which have percentage good more than 80% is considered for the analysis.

The in situ data are spaced irregularly and are converted to equidistant rectangular grids using VG Gridding for contouring and graphical display.

2.2 Satellite measurements

Wind datasets are acquired for the month of January 2009 and November–December 2011 from ASCAT (daily) aboard the EUMETSAT METOP satellite. Eight-day composite of the Ocean Color Level 3-binned product derived from MODIS Aqua in 4 km resolution acquired from GSFC NASA which is processed using SeaDAS is used to depict the chl-a patterns. TOPEX/POSEIDON (T/P) SSHA data (weekly composite) is obtained from CNES/NASA. The MODIS Aqua Level 3 Mapped SST data are derived from the NASA MODIS sensor onboard the Aqua satellite. The data have been mapped to a cylindrical equidistant map projection with 4.63 km spatial bins. Salinity is obtained from European Center for Medium range Weather Forecast Ocean Reanalysis System 4 (ECMWF ORAS4) on 1° × 1° grid and current data is taken from OSCAR (Ocean Surface Currents Analyses Real-time) on 0.33° grid.

Evaporation data is obtained from the Woods Hole Oceanographic Institution (WHOI) Objectively Analyzed air–sea Heat Fluxes (OAFlux) dataset on 1° × 1° grid. Precipitation data came from GPCP (Global Precipitation Climatology Project) version 1.3. Solar radiation flux is obtained from ESRL (Earth System Research Laboratory) NOAA 20th Century Reanalysis V2c.

The u and v components of the water velocity due to Ekman pumping are computed for the vertical column following Pond and Pickard (1983). The relation is explained as

$$u_E = V_0\cos\left(\frac{\pi}{4}+\frac{\pi z}{D_E}\right)\exp(\pi z/D_E), \quad v_E = V_0\sin\left(\frac{\pi}{4}+\frac{\pi z}{D_E}\right)\exp\left(\frac{\pi z}{D_E}\right) \tag{1}$$

$$V_0 = \frac{\sqrt{2}\pi\tau_{yn}}{D_E\rho f}, \quad \text{total Ekman current}, \tag{2}$$

$$D_E = \frac{4.3W}{(\sin\phi)^{\frac{1}{2}}}, \quad \text{Ekman depth}, \tag{3}$$

τ_{yn} is the magnitude of the wind stress on the sea surface, f is the Coriolis force, Φ is the latitude, and z is the water depth. At the sea surface, the surface current flows at 45° to the right of the wind direction in the northern hemisphere. Below the surface, the total current speed decreases as depth increases. When $z = -D_E$, at the Ekman depth, the direction of the flow becomes opposite to that at the surface.

The primary productivity (PP) of the region during the study was derived using Vertically Generalized Production Model (VGPM) of Behrenfeld and Falkowski (1997) which describes the relationship between the surface chlorophyll from satellite data and depth-integrated primary production. The VGPM is a chlorophyll-based model that estimates net primary production (NPP) from chlorophyll using a temperature-dependent description of chlorophyll-specific photosynthetic efficiency. In the VGPM, NPP is a function of chlorophyll, available light, and photosynthetic efficiency.

The core equation describing the relationship is expressed as

$$PP_{eu} = 0.66125P^B_{opt}\frac{E_0}{E_0+4.1}C_{SAT}\times Z_{eu}\times D_{IRR} \tag{4}$$

where C_{SAT} is the satellite surface chlorophyll concentration as derived from measurements of water leaving radiance (mg Chl/m^3). VGPM calculations of primary production were based on monthly average C_{SAT}. D_{IRR} is a daily photoperiod (in decimal hours) calculated for the middle of the month for each pixel, E_0 is the sea surface daily photosynthetically available radiation (PAR) (mol quanta/m^2/d), and Z_{eu} is the physical depth (m) of the euphotic zone defined as the penetration depth of 1% surface irradiance based on the Beer-Lambert law. Z_{eu} is calculated from C_{SAT} following Morel and Berthon (1989).

3 Results and discussion

The upper column dynamics can be best studied and illustrated based on the changes in the wind and SST pattern and the present study attempts on this approach considering the real-time in situ SST from CTD (bulk SST at 5 m) and scatterometer-derived wind fields for the observation time. Also, the hydrography can be best illustrated based on vertical profiles on temperature, salinity, and density and this has been addressed by analyzing the 91 and 44 castings during the two cruises.

3.1 Atmospheric forcing

The analyzed wind pattern suggested that the area is experienced with cold, dry continental air from northeast and the oceanic region is experienced with evaporative cooling with significant spatial variation (Wang et al. 2006). November–December 2011 characterizes northeasterly wind over the northern region and easterly winds in the southern region (6° to 9°N) with increasing magnitude towards south (Fig. 2a). However, during January 2009**,** the pattern is northeasterly over the entire area with magnitude increasing towards south as observed during November–December 2011 (Fig. 2b).

3.2 Upper layer mixing and hydrography

Immediate response due to atmospheric forcing will be best reflected in the sea surface temperature (SST) pattern and is thus considered as the most important parameter in the air-sea interaction processes (Manikiam 1988). November–December2011 is characterized with the prevalence of warmer water (≥ 28.4 °C) extended over the region and the temperature changed from 28.4 to 29.2 °C (Fig. 3a) which is quite different from the expected trend of increasing towards south (Rama Raju et al. 1981). East coast is somewhat cooler than the west, showing similar tendency during January 2009 (Fig. 4a). During January 2009, the SST recorded between 27.0 and 28.1 °C with warmer water in the south than the north. The waters along the east coast are comparatively cool in the range of 28.4–28.9 °C in the November–December 2011 and 27.3–27.6 °C in January 2009 than that along the west recording 28.5–29.2 °C in November–December 2011 and 27.6–28.1 °C in January 2009. North of Camorta is the coldest point in the November–December 2011 and the northeast in January 2009. The warmest point is northwest (29.2 °C) in November–December 2011 and southeast in January 2009.

From the SST maps, it is evident that the eastern side is more cool than the west. To explore this, the E-P (evaporation-precipitation) is calculated. During November–December 2011, the computed is negative in the southern latitude (up to 8°N) which ranges from $^{-}$101 to $^{-}$239 cm/year. E-P increases towards north vary from 16 to 158 cm/year. The eastern side is characterized with E-P of $^{-}$13–$^{-}$412 cm/year up to 6.5°N and again increases towards north like the western side (86–128 cm/year). For the period of January 2009, the western side E-P rate varies from $^{-}$33 to $^{-}$225 cm/year in the southern latitude (up to 6.5°N) and it increases towards north similar to November 2009 (47–179 cm/year). But in the eastern side, the E-P ranges from $^{-}$117 to $^{-}$215 cm/year up to 6°N and the value shoot up from 19 to 201 cm/year towards north. From this, it is evident that the eastern side is cooler than west due to the cold dry continental air from northeast which causes evaporation in the ocean surface.

During November–December 2011, the net solar radiation in the western part of the island chain varies from 160 to 280 W/m^2 and 71 to 260 W/m^2 in the eastern region. During January 2009, the western side receives solar radiation in the range of 142 to 278 W/m^2 and 82 to 258 W/m^2 in the eastern part. The cooling in the eastern side is due to the combined effect of evaporation and reduced solar radiation.

In the Andaman waters, the sea surface salinity (SSS) is low and falls in the range of 31.8–33.4 in November–December 2011 (Fig. 3b) and 32.05–33.25 in January 2009 (Fig. 4b) with significant spatial variation in the distribution pattern (Sewell 1929). Temperature-salinity (TS) profiles characterize two water types in the northeastern section as warm (27.5–29.0 °C) less saline (32.5–33.5) and less dense (20.2–21.5 kg/m^3) for the upper (5–55 m) and below this level, uniform waters occupied up to 1000 m. Similar trend exists for the southeast also with warm (24.5–29.3 °C), saline (32.3–34), and less dense water (20.5–23.4 kg/m^3) for the upper (5–80 m) column but the source of water occupying the upper layer is found to be different. For northeast, it is due to heavy runoff from Ayeyarwady-Salween river system, while intrusion of Malacca Strait water (Riley and Chester 1971) in the south defines the water mass (Rama Raju et al. 1981; Tan et al. 2006). Intrusion of low saline water through the Malacca Strait during the active winter as mentioned above is verified based on Levitus climatology for December and January. The western side of island chain exhibits more or less similar pattern and the area is shown to be occupied by BoB waters with temperature 25.0–29.2 °C, salinity 32.1–34.0, σ_t20.3–22.0 kg/m^3 in the upper column (5–75 m) and below with 5.0–24.9 °C, 34.0–34.9, and 22.1–27.3 kg/m^3 respectively up to 1000 m depth during December and January.

Satellite SST pattern during November–December 2011 (Fig. 5a) is observed with higher temperature in the northwest (29 °C) comparing to other parts in the Andaman waters. The

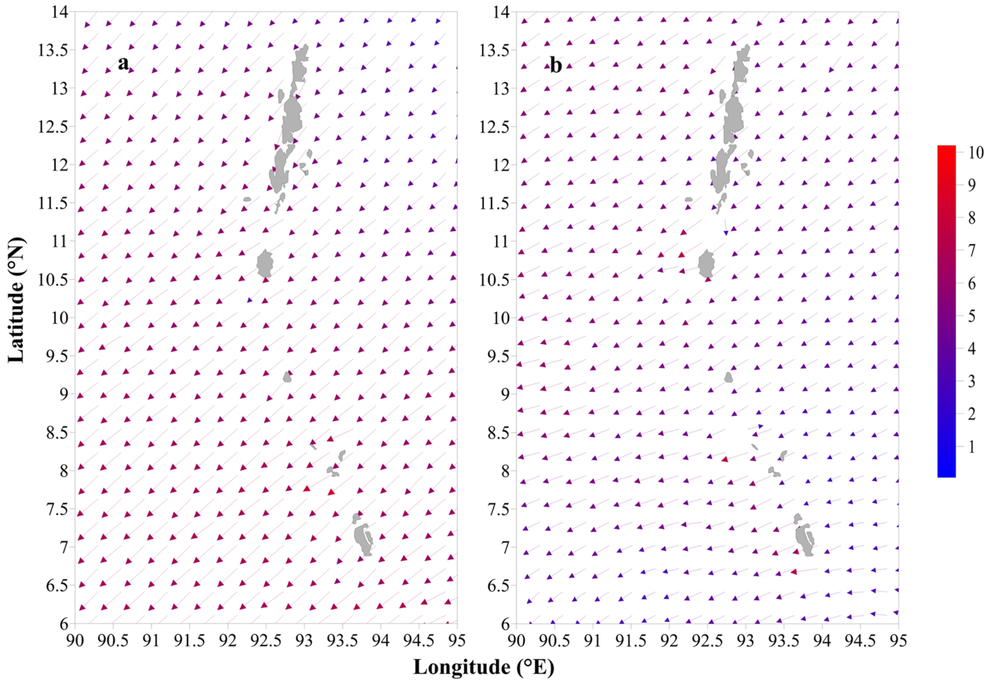

Fig. 2 Wind during **a** November–December 2011 and **b** January 2009

temperature decreases towards south (28°C) which is contrary to the winter trend of increasing towards south. Southeastern part is cooler than other parts. But in January 2009 (Fig. 5b), the SST changes from 27° C to 28° C with warmer water in the south. In situ SST shows quite similar trends with the satellite SST. The eastern side of the Andaman waters is cooler in November 2011, but in January 2009, the cooling trend is same in both sides of Andaman and Nicobar Islands.

The sea surface salinity from ECMWF during November–December 2011 (Fig. 6a) varies from 32 to 34 with higher salinity in the western side of the island chain comparing to east. January 2009 SSS ranges from 31.75 to 34, almost similar trend as November. During November, northeastern part is less saline due to the intrusion of Ayeyarwady-Salween river system. But in January 2009 (Fig. 6b), the southeastern side is occupied with less saline water due to the prevalence of less saline Pacific water through Malacca Strait. Even though the satellite products show spatio-temporal variability, the in situ data is well substantiated with satellite.

Surface Sigma-t also showed the same pattern of SSS and varies from 20.13 to 21.28 kg/m^3 with less dense water in the

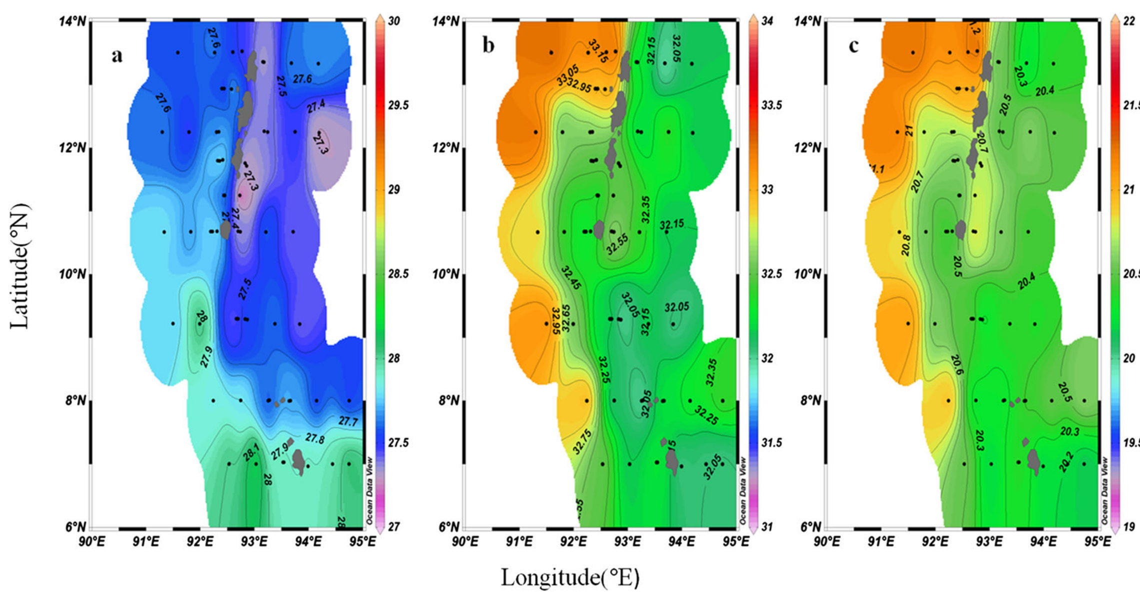

Fig. 3 Surface distribution of **a** temperature, **b** salinity, and **c** density during November–December 2011

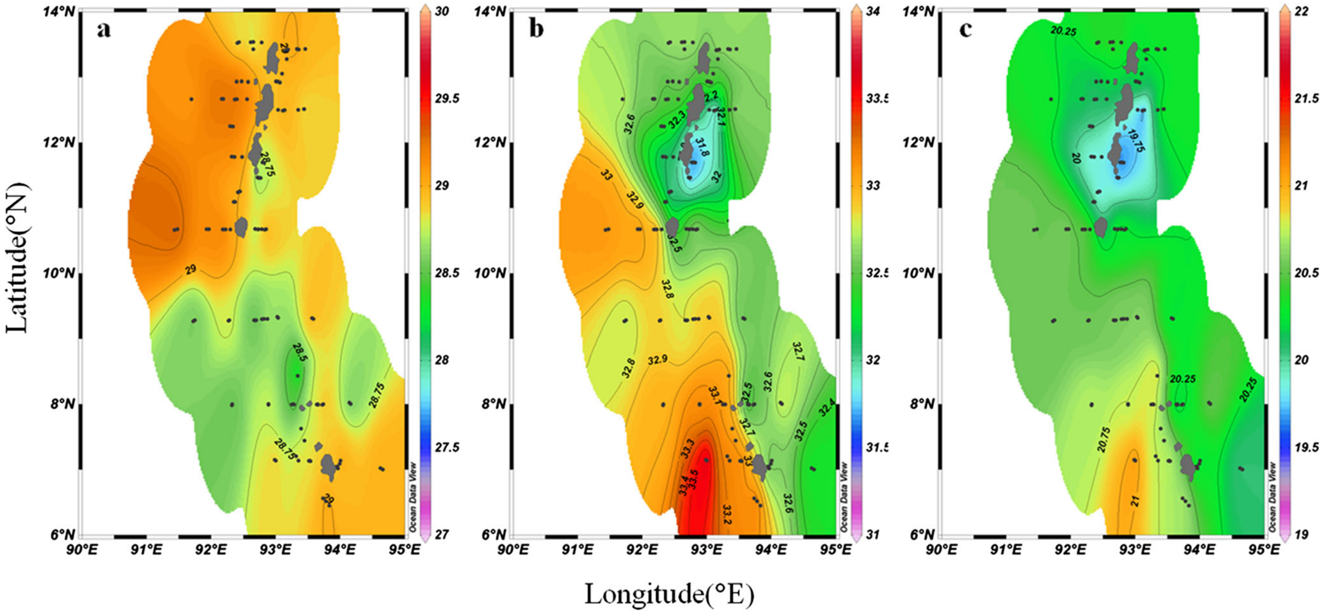

Fig. 4 Surface distribution of **a** temperature, **b** salinity, and **c** density during January 2009

east than the west in January 2009 (Fig. 4c). The density pattern of November–December 2011 (Fig. 3c) is entirely different from January 2009 and shows an increasing trend towards south (20.2–20.45 kg/m^3). Northeast part exhibits less density which is corroborated with SSS of the Ayeyarwady Region (Wyrtki 1971).

Further, the vertical distributions of temperature, salinity, and density are analyzed along the selected transects of north-south orientation and the physical parameters are found to be more or less uniform in the upper 50 m. The two cyclonic eddies were identified from SSHA altimetry, but we recorded in situ evidence for only one eddy which was encountered during November–December 2011 observation at 8°N and 92.5–93.5°E. The vertical temperature, salinity, and density profiles (Fig. 7a, b, c) show upsloping and it is prominent in the subsurface. Also, the MLD shoaled towards the coast from 47 to 19 m. The vertical current structure from ADCP (Fig. 8) confirms the presence of cyclonic eddy with directions northward (0.3 m/s) in the eastern part to southwestward (0.5 m/s) in the western part with magnitude decreasing towards depth.

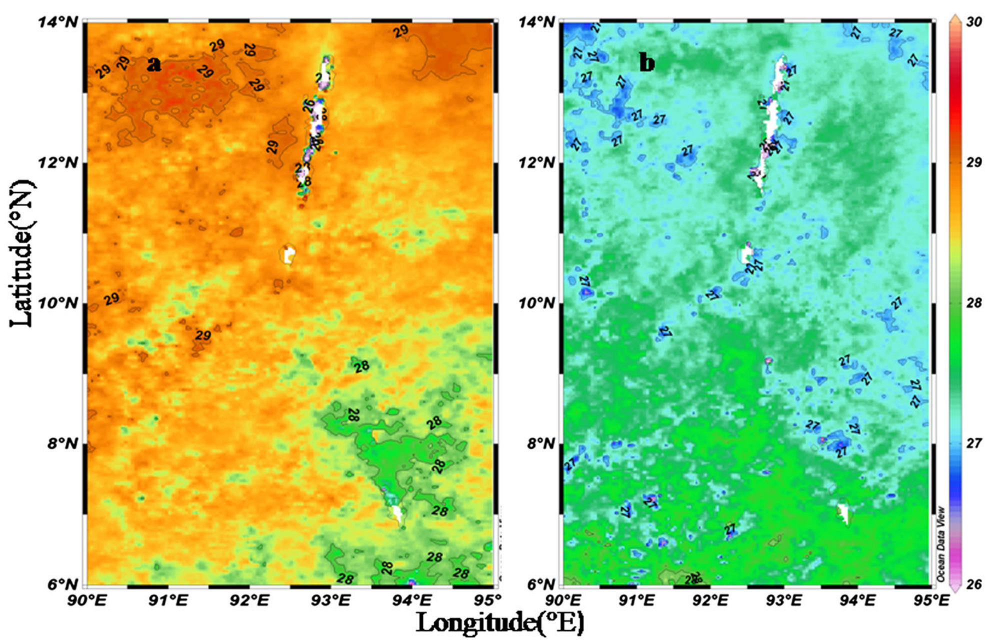

Fig. 5 Surface distribution of temperature from MODIS Aqua during **a** November–December 2011 and **b** January 2009

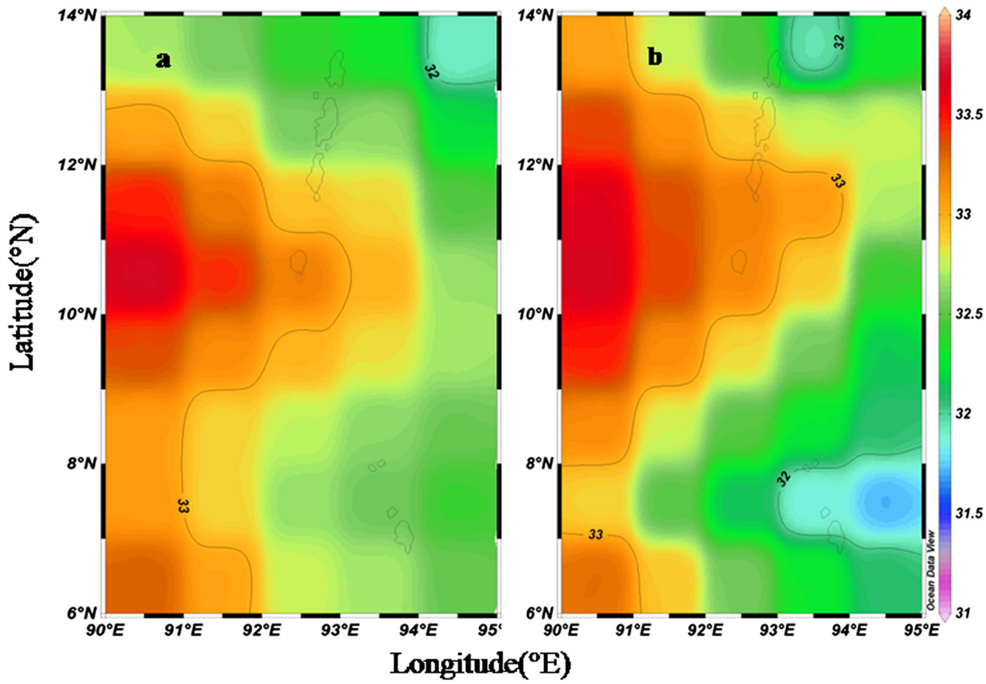

Fig. 6 Surface distribution of salinity from ECMWF during **a** November–December 2011 and **b** January 2009

Spatial variation in water properties thus subregionalizes the sea around Andaman into three, one is along the west, with BoB waters, second is at northeast with the influence of riverine discharge, and the third one is in south influenced by the intrusion of less saline water from Malacca Strait.

The extend of vertical mixing is determined by MLD and in the observation, it is found to be ranging between 20 and 44 m with high value at southwest in November–December 2011 (Fig. 9a) and 16 and 87 m with higher values at north in January 2009 (Fig. 10a). In November–December 2011, MLD in the western side of the island chain is 48 m at 7°N and shoals to 24 m at 9°N, again increases to 40 m at 10.5°N, and decreases towards north (24 m). In January 2009, MLD in the western side is about 17 m at 7°N, and it deepens to 42 m at 8°N. Again, along 8° to 10°N, it varies between 27 and 37 m. MLD shows sharp deepening north of 12°N with maximum value of 77 m at 13.8°N. In the eastern side of islands, MLD is shallow (20–32 m) in November–December 2011 and MLD maximum (72 m) is recorded at 11°N in the offshore waters of Middle and Little Andaman in January 2009. Along the southeast and southwest MLD is shallow and is in the range of 25–30 m in January 2009. From the time series analysis of wind speed in the coastal and oceanic region, the deepening of mixed layer is due to prevailing northeasterly winds and the wind-induced mixing. The shallow mixed layer in the east can be attributed to the presence of low saline water from Malacca Strait and Ayeyarwady-Salween river system which might have strengthened stratification resulting weak

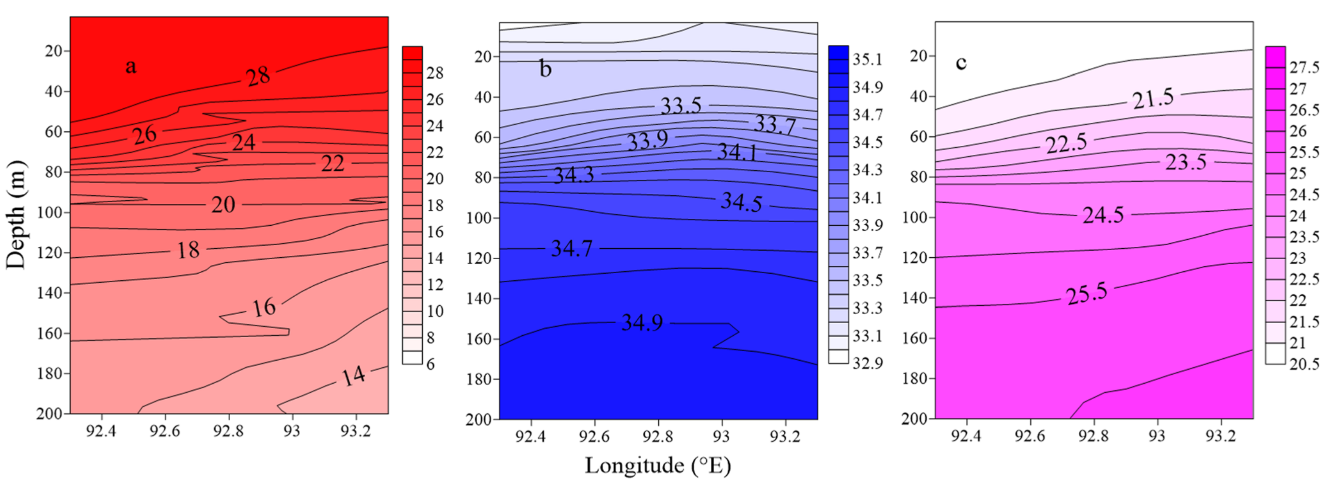

Fig. 7 Vertical profile of **a** temperature, **b** salinity, and **c** density at 8°N

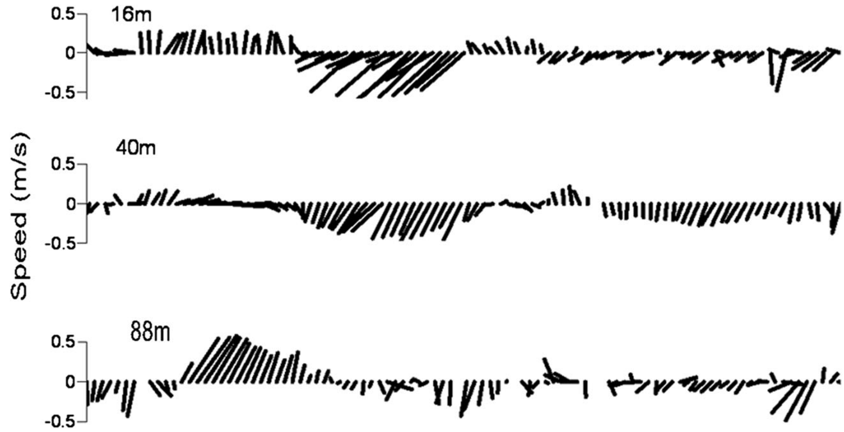

Fig. 8 Vertical current pattern at 8°N

vertical mixing (Rama Raju et al. 1981). In BoB also, the stratification is controlled by the freshwater flux, river runoff, mixing, and advection (Fousiya et al. 2015)

Another important observation noticed with the vertical distribution is the occurrence of temperature inversion (0.2–0.4 °C) in the upper subsurface layer (17–80 m). This is recorded in almost all the stations except around the Nancowry, Katchal, and Camorta Island chain in November–December 2011 and along the middle east Andaman in January 2009 and is significant as the subsurface values exceeded by 0.2 °C from that of surface as explained by Durand et al. (2004), and is a general feature of Andaman Sea during winter (Ramesh Babu and Sastry 1976).

Strong barrier layer is conducive for the formation of temperature inversion by suppressing the vertical advection processes (Masson et al. 2002). Presence of temperature inversion and shallow mixed layer indicates the existence of intermediate barrier layer, the layer between the base of mixed layer and the top of the thermocline (Lukas and Lindstrom 1991; Vinayachandran et al. 2002; Rao and Sivakumar 2003; Thadathil et al. 2007). Surface layer inversions observed at east may be due to differential mixing of Andaman waters with those coming from the adjacent seas and rivers as mentioned earlier. These low saline waters in conjunction with the intense evaporation contribute the above condition which supports the results from Rama Raju et al. (1981).

It is recorded by de Boyer Montégut et al. (2007) that the thermal inversion supported by barrier layer plays a significant role in warming the mixed layer during winter monsoon by entrainment of warm subsurface water. In support of these studies in the BoB, the present observations in the Andaman waters show that barrier layer is of 10–47 m thickness in November–December 2011 (Fig. 9b) and 10–50 m in January 2009 at most of the stations (Fig. 10b). It is more

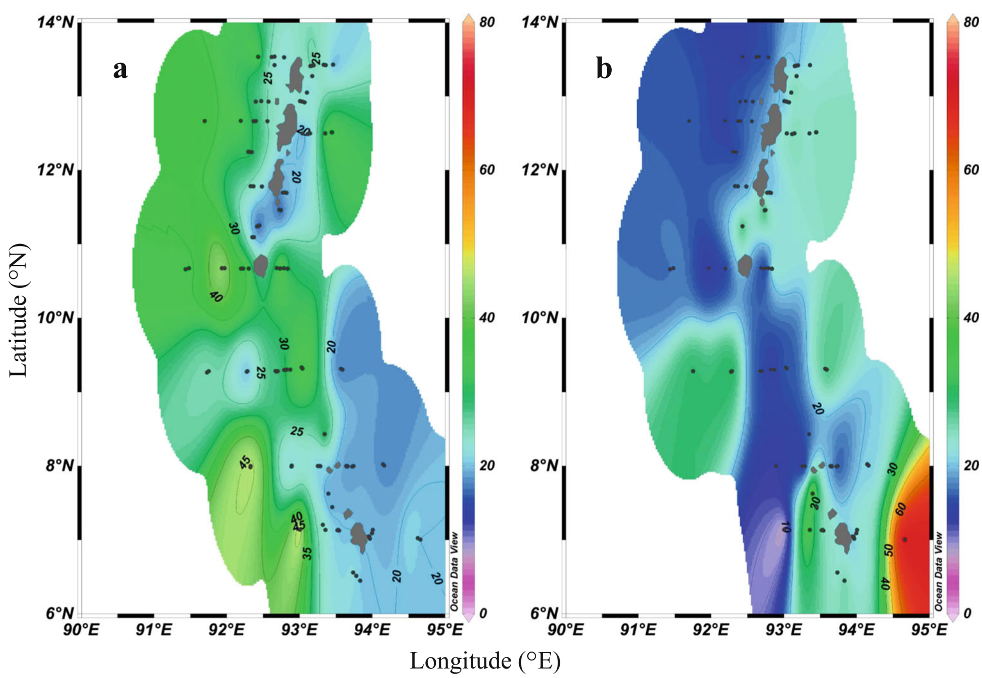

Fig. 9 **a** MLD, **b** BLT during November–December 2011

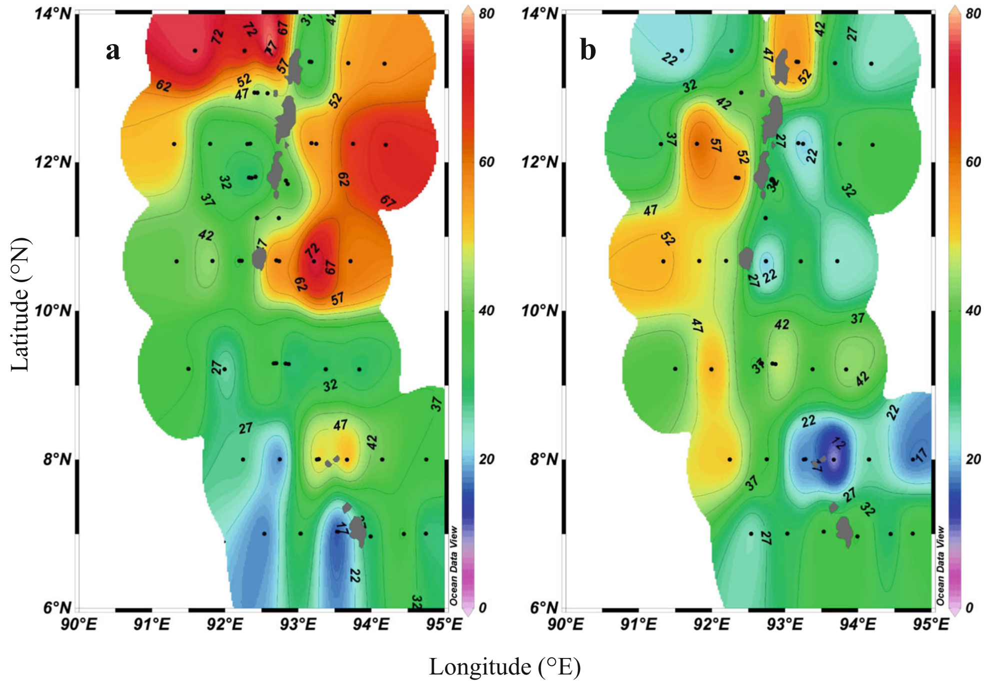

Fig. 10 **a** MLD, **b** BLT during January 2009

prominent in the southeastern side in November–December 2011 due to the presence of less saline Malacca water in the region. But in January 2009, barrier layer is more in the western side and in a small area along the eastern side of North Andaman Islands. The thickness of barrier layer is less in the northeastern side, which is a heavy freshwater input area as evidenced by the SSS values (32.05–33.25) and may be due to the soliton-induced mixing as reported by Osborne and Burch (1980). It is also observed that the sills and underwater volcanic seamounts in the eastern side of the islands are the potential source of internal waves in the region and contribute substantially to the upper layer mixing (Hyder et al. 2005).

The distribution pattern of barrier layer observed in the region is similar to the observations done by Thadathil et al. (2007), where they explored the seasonal variability of the barrier layer thickness and explained that the layer is more prominent in the Bay during winter monsoon. Also, the surface circulation and the redistribution of low saline (BoB water, freshwater from Ayeyarwady-Salween, and less saline South China Sea water from southeast) waters have shown a dominant influence on the distribution of barrier layer thickness (Agarwal et al. 2012). In addition, Ekman pumping and Rossby waves induced by coastal Kelvin waves propagating along the eastern boundary contribute significantly on the barrier layer thickness pattern (Girishkumar et al. 2011).

3.3 Upper layer circulation

The circulation pattern in the upper layer (16–96 m) is studied using the velocity profiles recorded through the VM ADCP of 76.8 kHz frequency. The analysis is done for different depths strata viz between 24 and 96 m in 8 m intervals. In November–December 2011, the current recorded at 16 m is considered for near surface pattern and this shows the presence of a strong (600–800 mm/s) eastward component from7°N to 8°N along the western side of the island chain (Fig. 11a). Above 8°N, it turns to northeastward direction away from the island chain with decreasing magnitude (200–300 mm/s). Further north (above 9°N), the flow is maintaining the same direction, i.e., northeastward, with a decreasing magnitude of ≤ 100 mm/s. Along the eastern side, the current is directed towards north and northeastward with reduced speed compared to western side of the island chain. At 32 m, the current shows same trend (Fig. 11b) like at surface. The data is analyzed for all 8 m cells up to 88 m depth (Fig. 11f) and found to follow the same pattern as that of near surface but with decreasing magnitude.

During January 2009, the current recorded at 24 m (Fig. 12a) represents near surface pattern and this shows the presence of a strong westward component of 600 mm/s up to 10°N along the western side of the island chain. South to 10°N, it takes southeastward direction towards the Nancowry, Katchal, and Camorta islands with magnitude in the range of 120–700 mm/s. Further south of 7°N, the flow is directed to south, with a strengthening in magnitude (700 mm/s). Along the eastern side, the observations indicate the flow from west to east through the Preparis Channel, which takes an anticyclonic path and reenter to the west via south of Car Nicobar. Overall, pattern is converging in the near surface layer between the latitudes 11–12°N and 93–94°E.

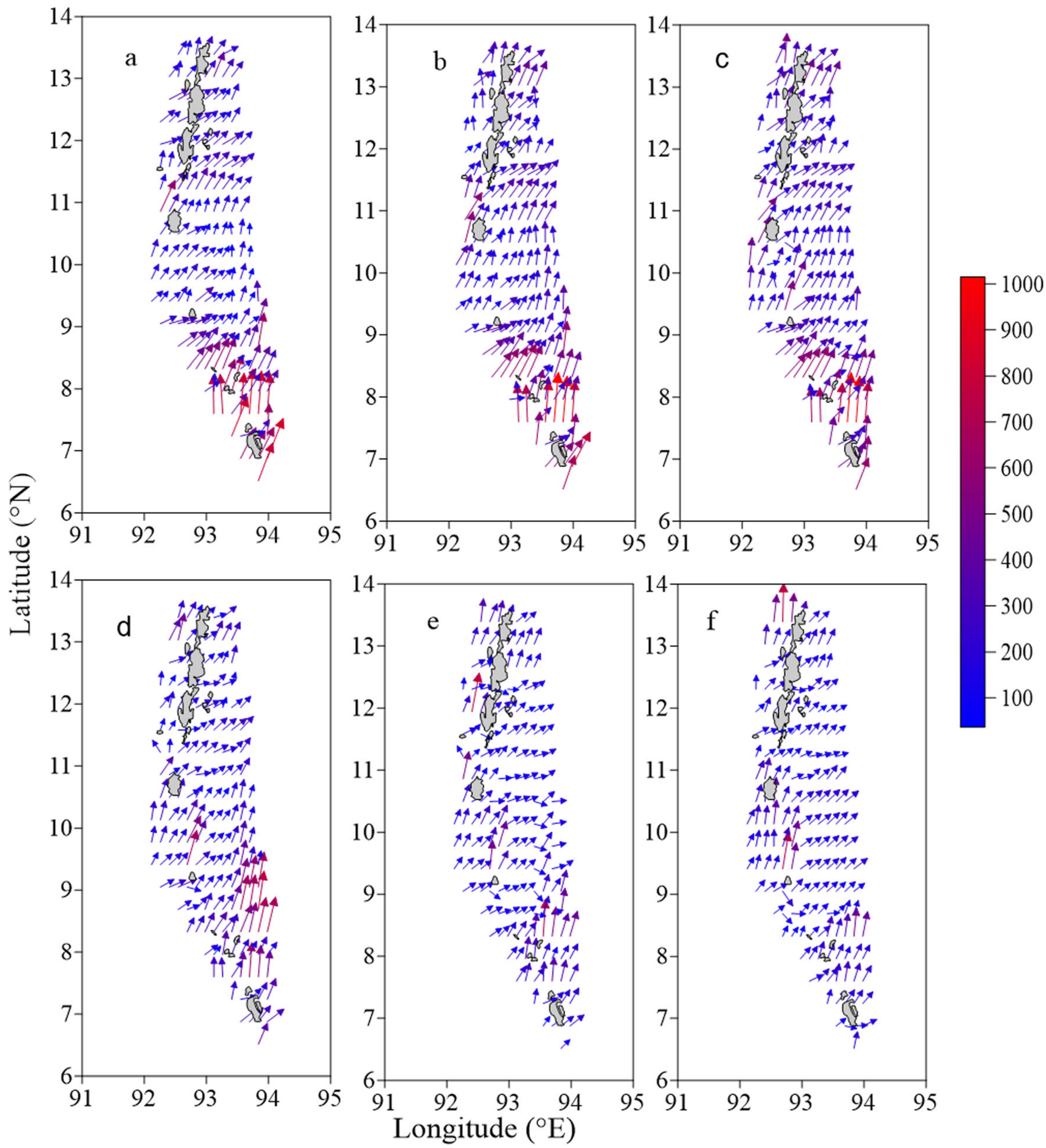

Fig. 11 Vertical section of current at **a** 16, **b** 32, **c** 40, **d** 56, **e** 72, and **f** 88 m in November–December 2011

At 32 m depth (Fig. 12b), the current pattern shows the same trend as that at the surface with magnitude in the range of 145–775 mm/s. The data is analyzed for all 8 m depth cells up to 96 m depth, and it is found that up to 80 m (Fig. 12e), the circulation is in the same pattern as that in the near surface layer. At this level, the magnitude strengthens to 1000 mm/s near to Car Nicobar Island. At 96 m depth (Fig. 12f), the current shows irregularity in its direction and the magnitude is maintained in almost the same range. The observations in the upper layer circulation suggest convergence of the water from east and west near the Nicobar and Little Nicobar islands.

During January 2009 (Fig. 13b), the surface pattern of current from OSCAR characterizes westward component of 200 mm/s from 5 to 10°N along the western side of the island chain. Further north of 10°N, cyclonic eddy is evident between 11 and 13°N. Westward component is prominent further north of 13°N. Along the eastern side, the flow in the eastern side of Andaman Islands between 12 and 14°N is purely northward and south of 12°N up to 8°N another cyclonic eddy like the western side of the Island chain is marked. Below 8°N, the flow is directed towards southwestward carrying the Malacca water. There is a clear indication of well-

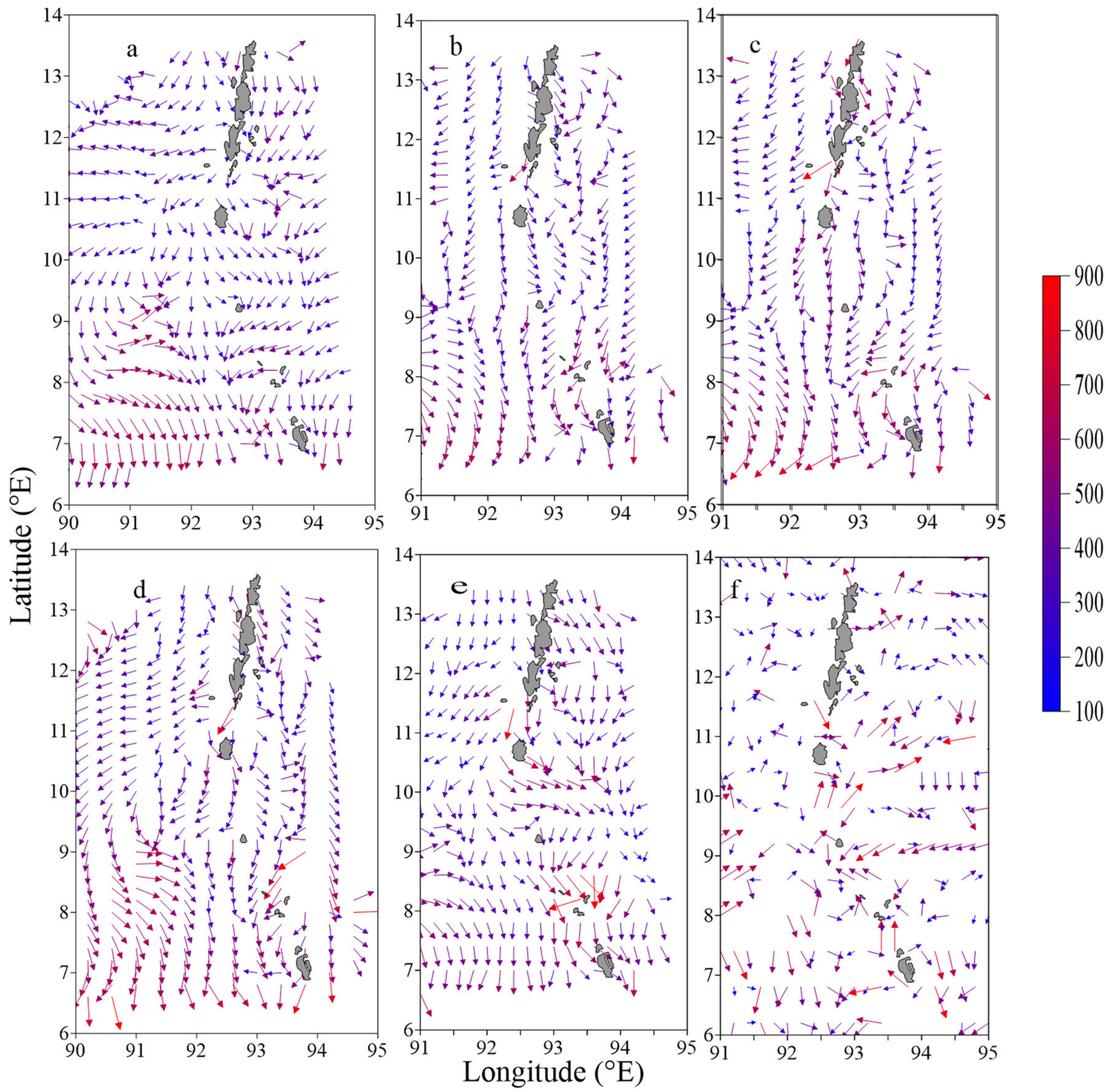

Fig. 12 Vertical section of current at **a** 24, **b** 32, **c** 40, **d** 56, **e** 80, and **f** 96 m in January 2009

organized northwestward currents of almost same magnitude (200 mm/s) up to 10°N.

In November and December (Fig. 13a), the surface circulation pattern in the western side of the island chain shows southwestward current between 6 and 7°N and further north between 7 and 10.5°N, anticyclonic circulation both in eastern and western part of the Islands. The anticyclonic pattern is also persist further north between 11 and 14°N. Northward current exists in western side of the island chain except the eddy region. The current shows the presence of a northwestward component of 200 mm/s up to 7°N and 96–98°E. This carries the productive water from Malacca Strait during winter monsoon which was also evidenced in the in situ ADCP current observations near to the island chain.

Another important aspect of understanding on seas surrounding the island chain is the island mass effect (IME), which may be reflected as a change in temperature/salinity/nutrient pattern, eutrophication due to terrigenous discharge, pollution, changes circulation pattern near the coast, coastal upwelling, and eddies. However, in the present study, the near coastal station considered is at 50 m depth contour and found no significant influence in hydrography except for silicate concentration, observed 2–10 μmol/L. However, no significant influence of the same is observed during the survey, except the high biovolume (0.55 ml/m^3) of zooplankton in the west. Other indications of the IME are the weak coastal upwelling observed in the chemical and biological response (Salini et al. 2010) and the irregularities in SSHA pattern as seen in Fig. 14c.

To further understand the forcing mechanism which controls the upper layer circulation of the region, the vertical extent of the momentum transfer due to Ekman depth is

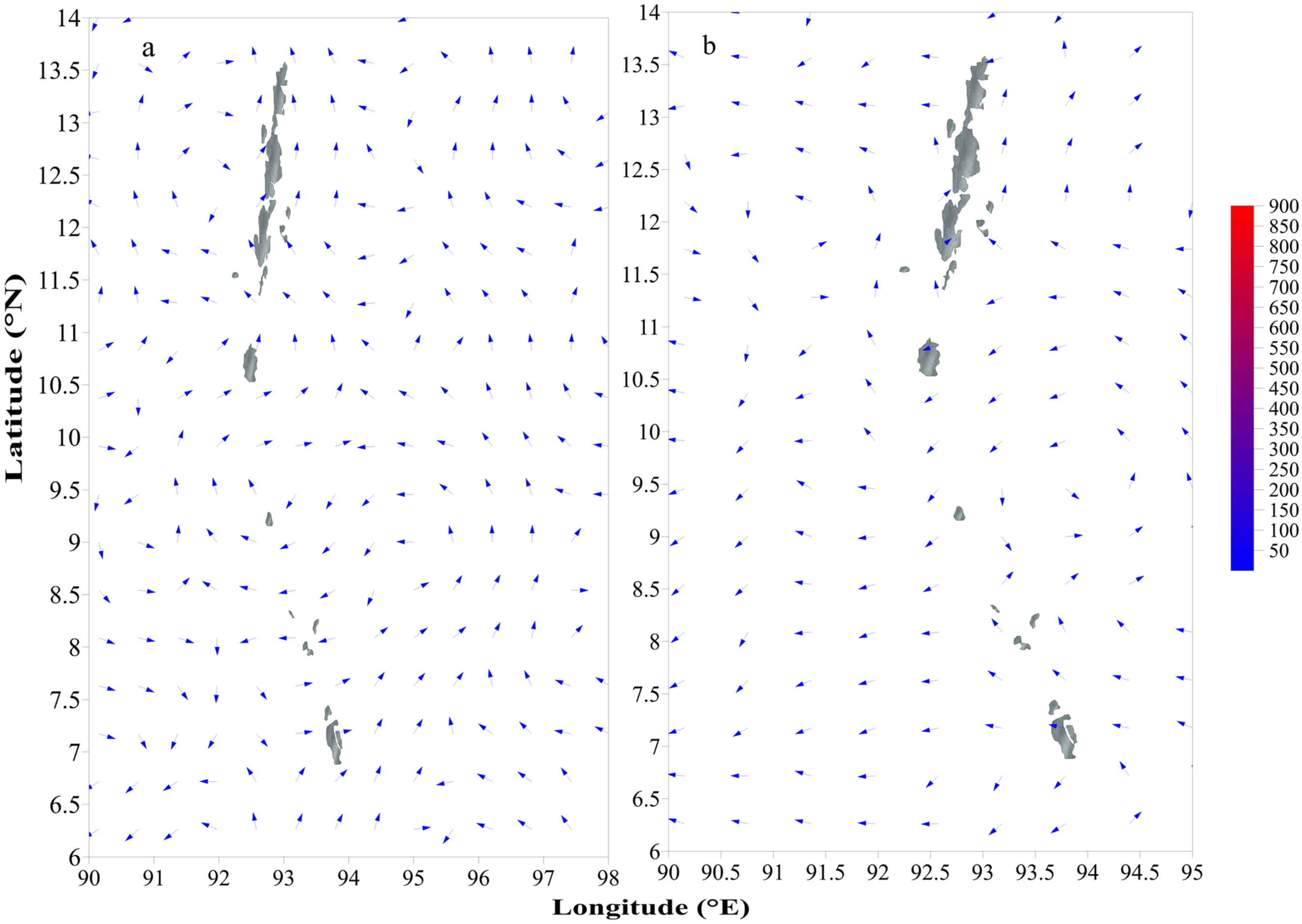

Fig. 13 OSCAR currents during **a** November–December 2011 and **b** January 2009

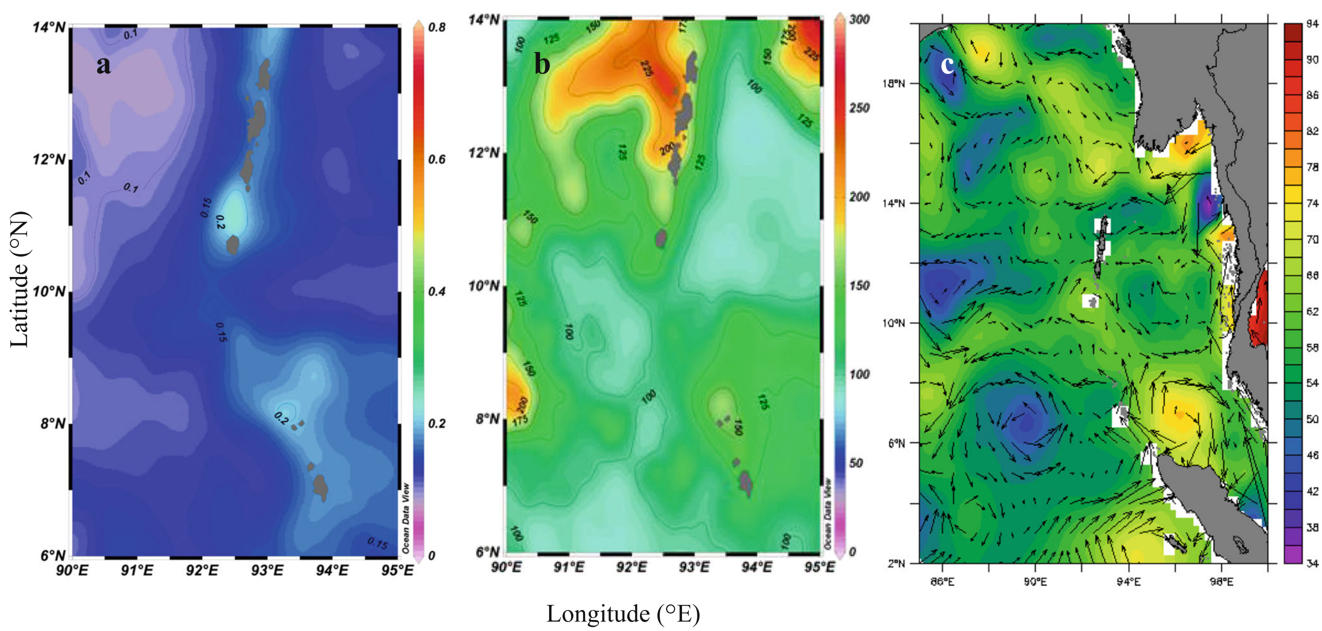

Fig. 14 Surface distribution of **a** chl-a (mg/m^3), **b** PP (mgC/m^2/d), and **c** SSHA and geostrophic currents during November–December 2011

computed using Pond and Pickard (1983) and on an average, it is 55 m in November–December 2011 and 52 m in January 2009. This strikes contradiction with the ADCP-derived current structure, which is uniform up to 88 m in November–December 2011 and 80 m in January 2009, and it explains that some other forcing is also involved other than the Ekman forcing. This supports the observation from Potemra et al. (1991) and Yang et al. (1998) that the propagation of Kelvin waves does play a major role in regulating the upper layer dynamics with clear seasonal variations. According to Chatterjee et al. (2017), the mean circulation within the Andaman Sea and around the islands is primarily driven by equatorial forcing, rather than the local wind forcing which is marginal. The current forced by local winds is weak compared to that remote forcing along the equator. So the present study, based on the in situ vertical profiles on currents and hydrographical parameters, suggests the role of additional factors than the atmospheric momentum transfer due to wind.

3.4 Biological response

Spatial and temporal changes in the physico-chemical characteristics of this region are expected to have great influence in the chl-a and phytoplankton distribution. Monthly composite of the surface chl-a derived from ocean color sensor is made use to understand the biological response and it is found that the mean surface chl-a varies between 0.1 and 0.4 mg/m^3 in November–December 2011 (Fig. 14a) and 0.2 and 0.4 mg/m^3 in January 2009 (Fig. 15a) with relatively higher concentration along the south of 10°N (> 0.3 mg/m^3) compared to other areas. The high concentration of surface chl-a may be due to the inflow from Malacca Strait. Rama Raju et al. (1981) reported the inflow of Malacca Strait into the southern region. The moderate chl-a (0.3–0.4 mg/m^3) along the coastal area is mainly due to the presence of the island chain. VGPM-derived column-integrated primary productivity (PP) shows variation between 100 and 225 mgC/m^2/d in November–December 2011 (Fig. 14b) and 200 and 300 mgC/m^2/d in January 2009 (Fig. 15b). Maximum PP is recorded as 300 mgC/m^2/d along the south in January 2009. At some extent, it spreads northward up to 9°N. Again, the higher chl-a and PP in the southeastern part are associated with productive environment of Malacca Strait. Weak mixing as explained in the upper layer mixing and hydrography between the surface, subsurface, and the bottom water may be the reason for low production in the Andaman Sea as suggested by Sengupta et al. (1981). Other than the near coastal area where PP > 250mgC/m^2/d and the southeastern part, the waters are more or less oligotrophic. However, the higher PP (150–200 mgC/m^2/d) during November–December 2011 in the southeastern and southwestern part is due to the cyclonic circulation, as evidenced from the SSHA pattern (Fig. 14c).

4 Conclusion

Physical forcing and related biological response of Andaman waters are addressed during winter monsoon (November–December 2011 and January 2009) based on in situ and satellite measurements. It is found that prevailing northerly and northeasterly winds make the area cool and, though not

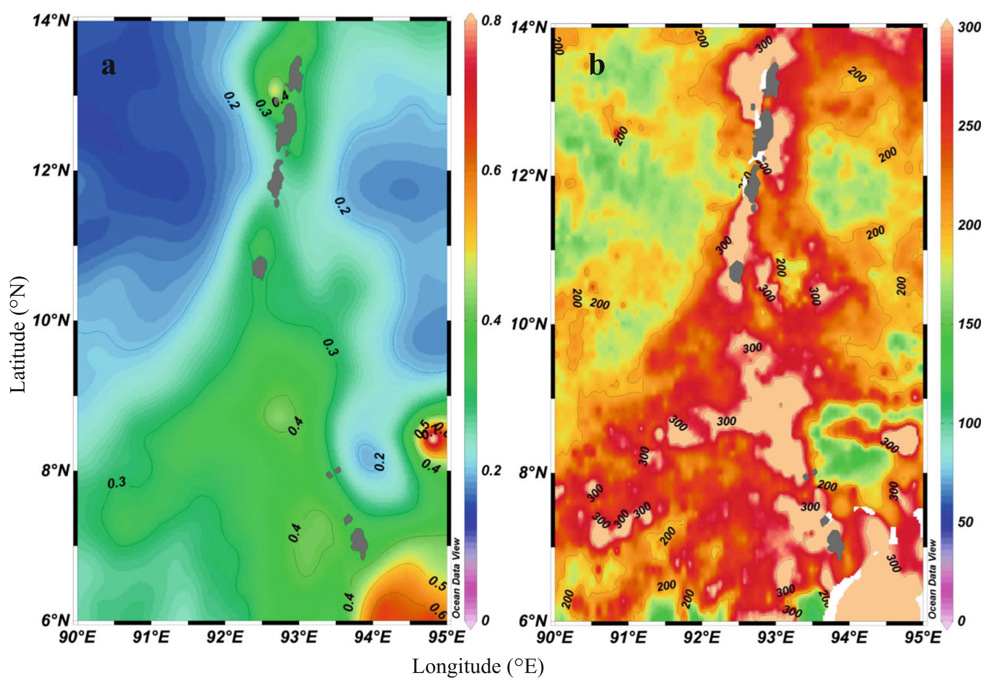

Fig. 15 Surface distribution of **a** chl-a (mg/m^3) and **b** PP (mgC/m^2/d) during January 2009

intense, influence the upper layer characteristics. Hydrography of the region clearly demarcates the area into three: (i) along west showing typical BoB characteristics, (ii) along east showing the influence of riverine input from Ayeyarwady-Salween river system supplemented with weak evaporative cooling, and (iii) south due to intrusion through Malacca Strait. Also, the study reports the upper layer circulation up to 96 m based on in situ current profiles as regulated by both geostrophy and Ekman in a magnitude range of 100–1000 mm/s. The southern area is productive compared to other parts due to the influence of productive environment of Malacca Strait. Overall, the region is oligotrophic in comparison with other seas in the Indian Ocean due to weak mixing between surface and subsurface water. The surface geostrophy and the production pattern evidence the role of local and remote forcing in determining the spatial pattern of oceanographic features of the region.

Acknowledgements Authors are grateful to the Ministry of Earth Sciences for supporting the work and for providing facilities onboard FORV Sagar Sampada for in situ measurements. All the fellow participants of the cruises FORV SS261 and SS292 are thankfully acknowledged. In situ data are obtained from FORV Data Centre in CMLRE. ASCAT Scatterometer wind field is obtained from NOAA/NESDIS. The TOPEX/Poseidon SSHA product is generated from the Merged Geophysical Data Record. Chlorophyll data was retrieved from GSFC NASA. This is CMLRE contribution ##.

References

Agarwal N, Sharma R, Parekh A, Basu S, Sarkar A, Agarwal VK (2012) Argo observations of barrier layer in the tropical Indian Ocean. Adv Space Res 50:642–654

Alpers W, Wang-Chen H, Hock L (1997) Observation of internal waves in the Andaman Sea by ERS SAR, Proc. 3rd ERS Symposium on Space at the Service of our Environment, Florence Italy, p 1287–1291

Behrenfeld MJ, Falkowski PG (1997) Photosynthetic rates derived from satellite-based chlorophyll concentration. Limnol Oceanogr 42:1–20

Bhattathiri PMA, Devassy VP (1981) Primary productivity of the Andaman Sea. Ind J Marine Sci 10:243–247

Biju A, Pillai HUK, Jayaraj KA, Sabu P, Muraleedharan KR (2010) Influence of environmental parameters on the vertical distribution and abundance of mesozooplankton in the Andaman waters during spring intermonsoon. In: Indian ocean marine living resources, book of abstracts, Centre of Marine Living Resources and Ecology, Ministry of Earth Sciences, Kochi, p 21

Chatterjee A, Shankar D, McCreary JP, Vinayachandran PN, Mukherjee A (2017) Dynamics of Andaman Sea circulation and its role in connecting the equatorial Indian Ocean to the Bay of Bengal. J Geophys Res: Oceans 122:3200–3218

de Boyer Montégut C, Vialard J, Shenoi SSC, Shankar D, Durand F, Ethe C, Madec G (2007) Simulated seasonal and interannual variability of mixed layer heat budget in the northern Indian Ocean. J Clim 20:3249–3268

Durand F, Shetye SR, Vialard J, Shankar D, Shenoi SSC, Ethe C, Madec G (2004) Impact of temperature inversions on SST evolution in the South-Eastern Arabian Sea during the pre-summer monsoon season. Geophys Res Lett 31:1–4

Fousiya TS, Parekh A, Gnanaseelan C (2015) Interannual variability of upper ocean stratification in Bay of Bengal: observational and modeling aspects. Theor Appl Climatol 126:285–301. https://doi.org/10.1007/s00704-015-1574-z

Geetha A, Kurup KN, Naomi TS, Soloman K, Mathew KJ (1997) Zooplankton abundance and secondary production in the seas around Andaman-Nicobar Islands. Ind J Fish 44:141–154

Girishkumar MS, Ravichandran M, McPhaden MJ, Rao RR (2011) Intraseasonal variability in barrier layer thickness in the south central Bay of Bengal. J Geophys Res 116

Hyder P, Jeans DRG, Cauquil E, Nerzic R (2005) Observation and predictability of internal solitons in the northern Andaman Sea. J Appl Ocean Res 27:1–11

Ibrahim Z, Yanagi T (2006) The influence of the Andaman Sea and the South China Sea on water mass in the Malacca Strait. Mer 43(44):33–42

Kamesh Raju KA, Ramprasad T, Rao PS, Rao BR, Varghese J (2004) New insights into the tectonic evolution of the Andaman Basin Northeast Indian Ocean. Earth Planet Sci Lett 221:145–162

Kara AB, Rochford PA, Hurlburt HE (2000) An optimal definition for ocean mixed layer depth. J Geophys Res 105:803–821

Lalithambika Devi CB, Rosamma S, Aravndakshan PN, Meenakshikunjamma PP (1996) Ichthyoplankton from Andaman and Nicobar seas. Proceedings of Second Workshop Scientific Results of FORV Sagar Sampada, p 239–248

Lukas R, Lindstrom E (1991) The mixed layer of the western equatorial Pacific Ocean. J Geophys Res 96:3343–3357

Manickasundaram M, Ramaiyan V (1990) On some fish eggs and larvae from the Andaman and Nicobar seas. Proceedings of First Workshop Scientific Results of FORV Sagar Sampada, p 193–199

Manikiam B (1988) Remote Sensing Techniques for Ocean-related studies. Current Science 57:764–767

Masson S, McCreary P, Kohler K (2002) A model study of the seasonal variability and formation mechanisms of the barrier layer in the eastern equatorial Indian Ocean. J Geophys Res 107:18–20

Morel A, Berthon J (1989) Surface pigments, algal biomass profiles, and potential production of the euphotic layer: relationships reinvestigated in view of remote-sensing applications. Limnol Oceanogr 34:1545–1562

Murthy CS, Das PK, Gouveia AD (1981) Some Physical aspects of the waters around the Little Andaman Island. Indian Journal of Marine Sciences 10:221–227

Nair VR, Gireesh R. (2010) Biodiversity of chaetognaths of the Andaman sea. Indian Ocean. Deep Sea Research II 57:2135–2147

Nienhaus MJ, Subrahmanyam B, Murty VSN (2012) Altimetric Observations and model simulations of Coastal Kelvin waves in the Bay of Bengal. Mar Geod 35:190–216

Osborne AR (1990) The generation and propagation of internal solitons in the Andaman Sea. In: Fordy AP (ed) Soliton theory: a survey of results. Manchester University Press, Manchester, pp 152–173

Osborne AR, Burch TL (1980) Internal solitons in the Andaman Sea. Science 208:451–460

Pillai HUK, Jayaraj KA, Rafeeq M, Jayalakshmi KJ, Revichandran C (2011) Mesozooplankton distribution near an active volcanic island in the Andaman Sea (Barren Island). Environmental Monitoring and Assessment 176:239–250

Pond S, Pickard GL (1983) Introduction to dynamical oceanography, 2nd edn. Woburn, Butterworth-Heinemann Ltd

Potemra JT, Luther ME, O'Brien JJ (1991) The seasonal circulation of the upper ocean in the Bay of Bengal. J Geophys Res 96:667–683

Rama Raju DV, Gouveia AD, Murthy CS (1981) Some physical characteristics of Andaman Sea waters during winter. Ind J Marine Sci 10:211–218

Ramaswamy V, Rao PS, Rao KH, Thwin S, Rao NS, Raiker V (2004) Tidal influence on suspended sediment distribution and dispersal in the northern Andaman Sea and Gulf of Martaban. Mar Geol 208:33–42

Ramesh Babu V, Sastry JS (1976) Hydrography of the Andaman Sea during late winter. Ind J Marine Sci 5:179–189

Rao RR, Sivakumar R (2003) Seasonal variability of sea surface salinity and salt budget of the mixed layer of the north Indian Ocean. J Geophys Res 108:1–13

Riley JP, Chester R (1971) Introduction to marine chemistry. Academic press. Inc. Ltd, London, p 465

Robinson RAJ, Bird MI, Oo NW, Hoey TB, Aye MMD, Higgitt L, Lud XX, Swe A, Tun T, Win SL (2007) The Irrawaddy river sediment flux to the Indian Ocean: the original nineteenth-century data revisited. J Geol 115:629–640

Rosamma S, Meenakshikunjamma PP (1996). Ostracods of Andaman Sea. Proceedings of Second Workshop Scientific Results of FORV Sagar Sampada, p 197–203

Salini TC, Fanimol CL, Smitha BR, Jayalakshmi KJ, Asha Devi CR, Sanjeevan VN, Saravanane N, Sajeev R (2010) Oceanography of the Andaman waters: Physico-chemical and biological characteristics during January 2009. In: GVM G et al (eds) Indian Ocean marine living resources, book of abstracts. Centre for Marine Living Resources and Ecology, Ministry of Earth Sciences, Kochi, p 29

Sarupriya JS, Bhargava RMS (1993) Seasonal primary production in different sectors of the EEZ of India. Mahasagar 26:139–147

Sengupta R, Moraes C, George MD, Kureishy TW, Noronha RJ, Fondekar SP (1981) Chemistry and hydrography of the Andaman Sea. Ind J Marine Sci 10:228–233

Sewell RBS (1929) Geographic and oceanographic research in Indian waters, Part V. Temperature and salinity of surface waters of the Bay of Bengal and Andaman Sea, with references to the Laccadive Sea. Memoirs of the Asintic Soc Bengal 9:207–355

Sprintall SR, Tomczak M (1993) Evidence of the barrier layer in the surface layer of the tropics. J Geophys Res 97:7305–7316

Tan CK, Ishizaka J, Matsumura S, Yusoff FM, Mohamed MIH (2006) Seasonal variability of SeaWiFS chlorophyll a in the Malacca Straits in relation to Asian monsoon. Cont Shelf Res 26:168–178

Thadathil P, Muraleedharan PM, Rao RR, Somayajulu YK, Reddy GV, Revichandran C (2007) Observed seasonal variability ofbarrier layer in the Bay of Bengal. J Geophys Res 112

Unnikrishnan AS, Bahulayan N (1991) Simulation of barotropic wind-driven circulation in the Bay of Bengal and Andaman Sea during premonsoon and postmonsoon seasons. Ind J Marine Sci 20:97–101

Varkey MJ, Murty VSN, Suryanarayana A (1996) Physical oceanography of Bay of Bengal and Andaman Sea. Oceanography and marine biology: an annual review. University College London Press, p 1–70

Vinayachandran PN, Murty VSN, Ramesh Babu V (2002) Observations of barrier layer formation in the Bay of Bengal during summer monsoon. J Geophys Res 107

Wang B, Webster P, Kikuchi K, Yasunari T, Qi Y (2006) Boreal summer quasi-monthly oscillation in the global tropics. Clim Dyn 27:661–675

Wyrtki K (1971) Oceanographic Atlas of the International Indian Ocean Expedition. National Science Foundation, Washington, p 531

Wyrtki K (1973) Physical oceanography of the Indian Ocean. Chapman and Hall Ltd., London, pp 18–37

Yang J, Yu L, Koblinsky CJ, Adamec D (1998) Dynamics of the seasonal variations in the Indian Ocean from TOPEX/POSEIDON sea surface height and an ocean model. Geophys Res Lett 25:1915–1918